



Gazi University

**Journal of Science**

PART A: ENGINEERING AND INNOVATION

<http://dergipark.org.tr/guj.1259370>

## Investigation of Mechanical Properties of Aluminum 7075 Alloy via Surface Engineering

Gözde ALTUNTAŞ<sup>1\*</sup> Gamze YAZBAHAR<sup>2</sup> Bülent BOSTAN<sup>1</sup> <sup>1</sup>Gazi University, Faculty of Technology, Department of Metallurgical and Materials Engineering, Ankara, Türkiye<sup>2</sup>Gazi University, Institute of Science and Technology, Ankara, Türkiye

Keywords	Abstract
Micro Arc Oxidation (MAO)	In this study, MAO process, which is one of the surface coating methods, was applied to 7075-T6 Al alloy in a thin thickness and the relationship between its mechanical properties compared to its uncoated state was investigated. Surface microstructure images of the prepared samples, coating thickness from the cross section and eds analysis were measured by scanning electron microscope (SEM). With the XRD analysis, the peaks in the material on which the coating is made were determined and the difference was examined according to the uncoated state. How the coating affects the dislocation density was investigated. The microhardness value of the samples, which were coated with 2 µm MAO from the surface, was measured according to HV 0.5. The hardness value was thus increased by 50%. The weight loss of coated and uncoated materials was calculated. Despite such a thin coating, the wear resistance has increased approximately 8 times compared to the uncoated state.
7075 Al alloy	
Wear	
Dislocation Density	

### Cite

Altuntaş, G., Yazbahar, G., & Bostan, B. (2023). Investigation of Mechanical Properties of Aluminum 7075 Alloy via Surface Engineering. *GU J Sci, Part A, 10(2)*, 157-165. doi:10.54287/guj.1259370

Author ID (ORCID Number)	Article Process
0000-0003-4504-0850	<b>Submission Date</b> 02.03.2023
0000-0002-4085-4786	<b>Revision Date</b> 27.03.2023
0000-0002-6114-875X	<b>Accepted Date</b> 03.04.2023
	<b>Published Date</b> 15.06.2023

## 1. INTRODUCTION

Aluminum alloys are widely used in areas such as aviation and space due to their high strength and low density properties (G. Altuntaş et al., 2021). It is also a material group that can compete with steels (O. Altuntaş & Güral, 2015). 7075, an aluminum alloy, is extensively used due to its high strength (O. Altuntaş, 2022). The naturally occurring aluminum oxide film on the surface of the aluminum alloy cannot protect the matrix for a long time (Li et al., 2019).

It is known that some coatings applied to aluminum alloy are effective in improving hardness, corrosion and wear. One of these methods, MAO, is an electrochemical plasma treatment that creates oxide ceramic coatings on light metals (Dean et al., 2015). The MAO process is also referred to by many names in the literature, such as spark anodic oxidation, micro plasma oxidation or plasma electrolytic oxidation. In this process, there is an electrolytic cell, the metal to be oxidized in the anode part, a metal such as stainless steel in the cathode part, a suitable solution that provides ion transport and oxidation, and a cooling system with a power source. The passive oxide layer is broken with the applied high voltage and a much thicker oxide layer is obtained at very high voltage values. For example, when aluminum is exposed to micro arc oxidation, oxides such as  $\alpha$  and  $\gamma$  alumina can be formed. According to traditional anodic oxidation, MAO is more reliable and does not contain heavy metal elements (Baxi et al., 2008). Ceramic coatings produced with MAO coating exhibit good adhesion to the substrate, high wear resistance and corrosion resistance (Yilmaz et al., 2021). Characteristics of ceramic coatings are mainly affected by the factors with electrolyte composition and current density (Sundararajan & Krishna, 2003). It is also known that the microhardness of micro arc films decreases with increasing depth

\*Corresponding Author, e-mail: [gozdealtuntas@gazi.edu.tr](mailto:gozdealtuntas@gazi.edu.tr)

from the interface to the coating surface (Qi et al., 2022). The performance of micro arc coatings depends on their chemical structure, composition and porosity. To improve the properties of micro-arc coatings, the mechanism of micro-discharge formation during micro-arc operation should be known (Song & Shi, 2014). Various organic compounds and other special chemical additives are used during MAO coatings by modifying the electrolyte solution to impart the desired qualities, especially better corrosion resistance (Zhang et al., 2023). Considering the high performance of the MAO coating, this process still has great potential application and therefore many researchers are making significant efforts to reduce or close the micropores to further improve the corrosion resistance it offers. (Shen et al., 2023). In a study that applied MAO to 7075 aluminum alloy; All samples treated with MAO showed better corrosion and wear resistance compared to the substrate.

In this study, the effect of MAO on the mechanical properties of Al 7075-T6 alloy was investigated in a very thin thickness. With the thin coating, the cost was reduced and the hardness value increased by approximately 50%. The abrasion resistance of the coated sample was improved 8 times on average.

## 2. MATERIAL AND METHOD

In the experimental study; 7075 aluminum sheet material was purchased. The chemical composition of the material is given in Table 1. The uncoated material was designated S.

**Table 1.** Chemical composition of the material (% weight)

ELEMENTS (%)						
Mg	Zn	Cr	Cu	Fe	Si	Al
2,61	5,7	0,175	1,72	0,14	0,063	Balance

Prior to MAO treatment, 7075 Al/T6 alloy was sanded successively with 400#, 600#, 800# and 1200# SiC sandpapers to achieve average surface roughness. It was then ultrasonically cleaned with ethanol and deionized water for 5 minutes. Finally, it was dried with nitrogen. Before the coating process, the frequency, voltage and time parameters effective on the MAO process were determined as constant. In the MAO process, the frequency value was applied at 1000 Hz. The positive and negative voltages applied to the process were applied over 420V and 100V, respectively, and the positive duty cycle (Duty Cycle) was studied at 20% negative duty cycle 5%. In the experimental process, 7075-T6 aluminum alloy sample was chosen as the anode and the stainless steel bath wall as the cathode. During the process, the electrolyte was mixed and cooled with cooling water passed through the bath wall so that it does not rise to a temperature above 30°C. Then, the coated 7075-T6 aluminum alloy samples, which were treated with MAO, were washed with distilled water and alcohol and dried. This sample is coded as SM. Figure 1 shows the schematic of the hardware used in the MAO process.

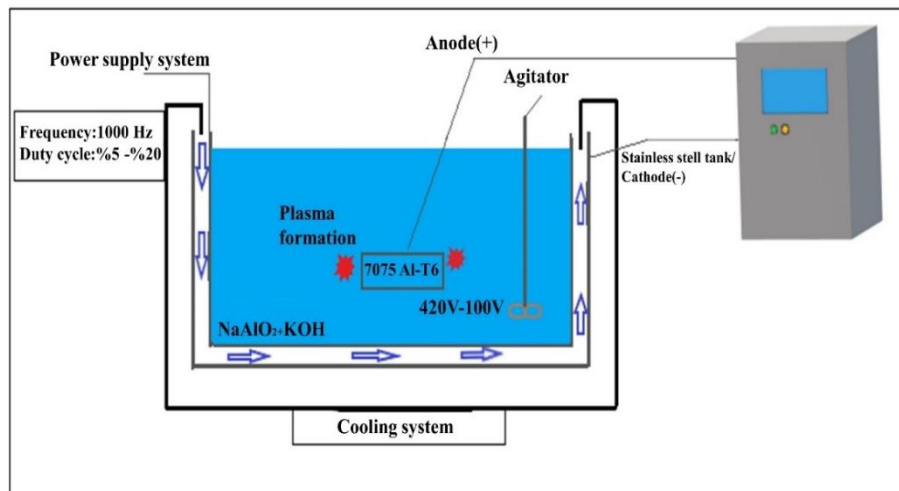
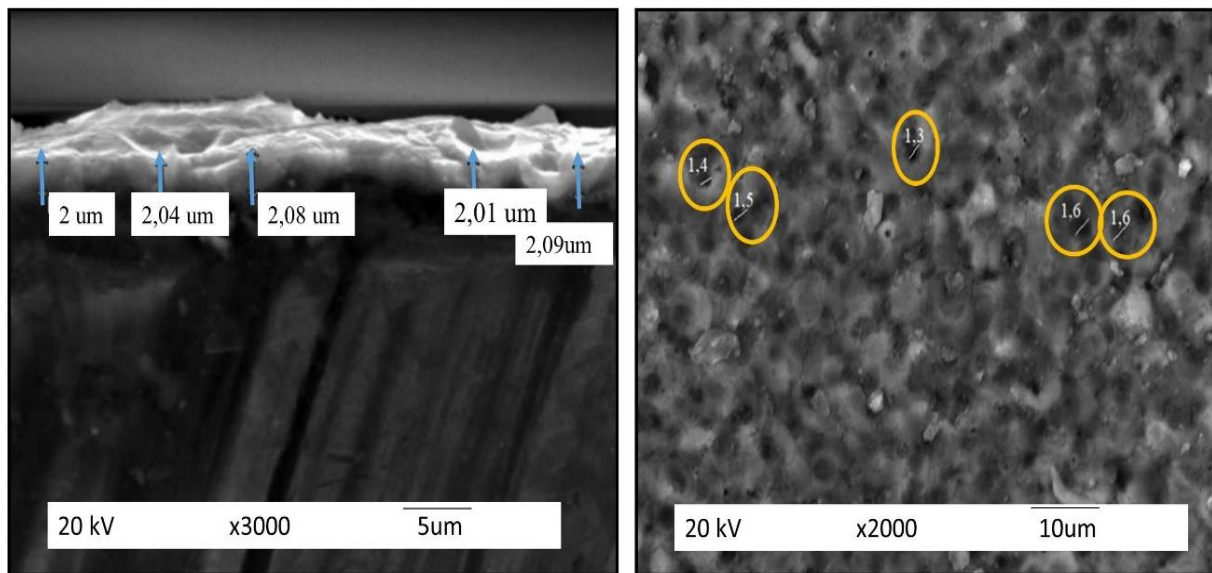


**Figure 1.** Schematic representation of the equipment used in the MAO process

Surface microstructure and element analysis of MAO coatings were examined using the JSM-6060LV scanning electron microscope (SEM). Coating thickness was measured from SEM cross-section images of MAO samples. In addition, ImageJ software was used to measure the porosity of the MAO coatings. The micro hardness of the samples was measured in QNESS Hardness device according to HV0.5. The friction and wear behavior of the samples were evaluated with a wear tester (Turkyus) under dry sliding condition. For the wear test, loads were selected as 5N, 10N, 15N respectively.

### 3. RESULTS AND DISCUSSION

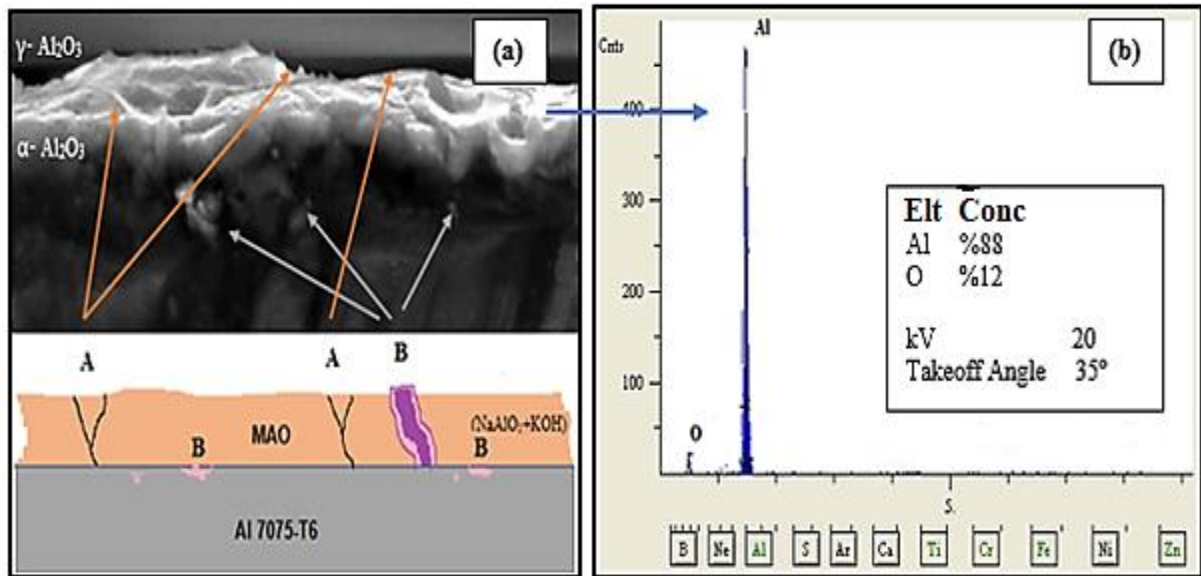
The coating thickness and surface appearance of the sample coated with MAO are shown in Figure 2a. It is understood that the coating is carried out in a homogeneous way. It is seen that the coating thickness on the surface is about 2µm. In Figure 2b, the diameters of the porosities on the surface were measured with the Image J image software program (Schneider et al., 2020). Measurements at 5 points were measured as 1.4µm, 1.5µm, 1.3µm, 1.6µm and 1.6µm, respectively. Average porosities were calculated as 1.48µm. Increasing the voltage while coating increases the thickness of the coating and also increases the diameter of the porosities (Sobolev et al., 2020).



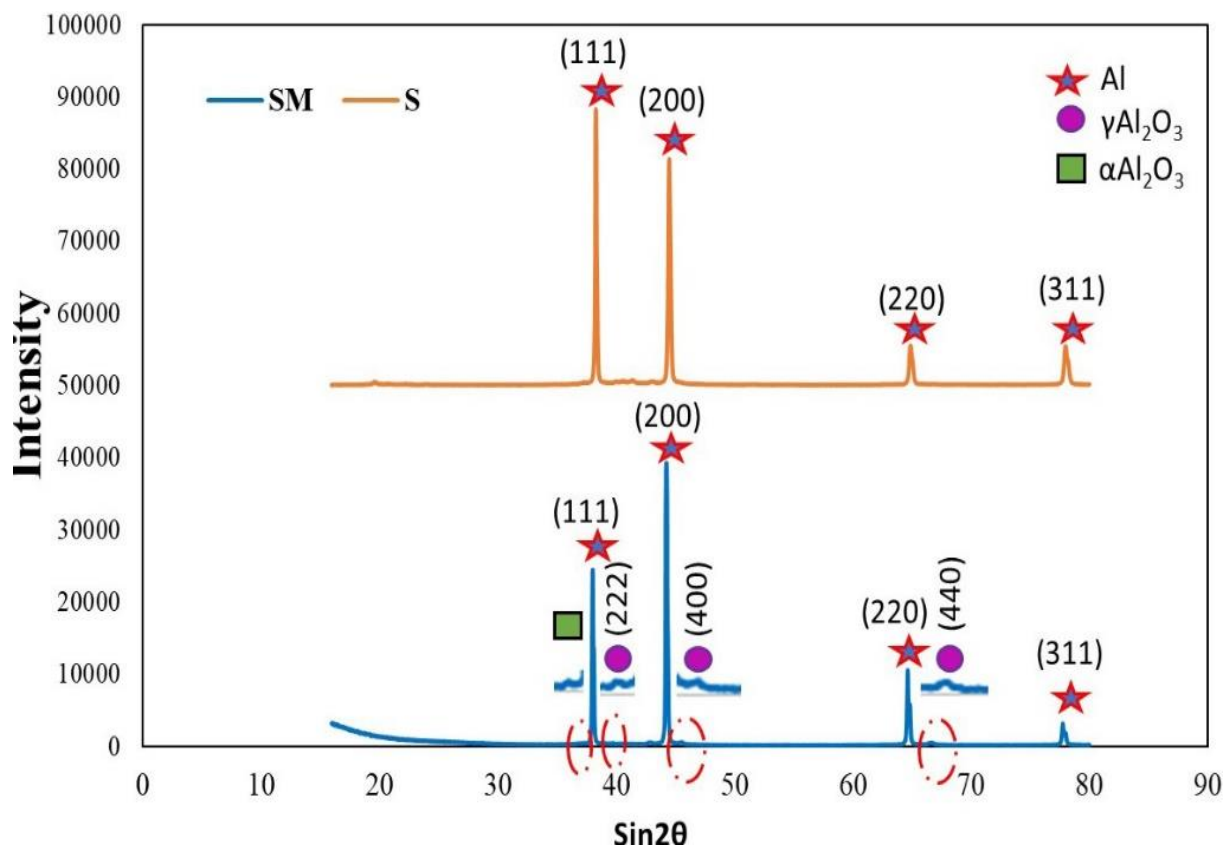
**Figure 2.** a) Cross-sectional SEM image of SM sample b) Surface SEM image of SM sample

Figure 3 shows the EDS analysis of the coating region. Type B discharge consists of regional high electric field density produced during the process. Type A discharges, on the other hand, occur as gas discharges within the micropores on the surface. A-type discharges, on the other hand, create small and large pores on the surface because they occur in micropores close to the surface and have lower energy than B-type discharges. As a result of the oxidation of the base metal in type B discharges, the metal's oxide grows inwards, while in type A discharges, oxides containing electrolyte components grow outward as the existing oxide and molten metal react with the electrolyte components (Hussein et al., 2013). With the rapid solidification of  $\text{Al}_2\text{O}_3$  during the coating process, metastable  $\gamma\text{-Al}_2\text{O}_3$  phase formation begins. As the coating surface comes into contact with the electrolyte, it cools quickly and  $\gamma\text{-Al}_2\text{O}_3$  is formed in the outer surface layer. (Figure 3). However, due to the low thermal conductivity of alumina, the main layer of the coatings remains hot because the heat cannot be easily dissipated. Therefore, the outer surface layer changes from  $\gamma\text{-Al}_2\text{O}_3$  to  $\alpha\text{-Al}_2\text{O}_3$ . Thus, the expected  $\alpha\text{-Al}_2\text{O}_3$  continues to increase up to the coating-material interface (Xin et al., 2006).

Figure 4 shows the XRD analysis of 7075-T6 Al alloy (S) and MAO (SM) coating. In the S sample, the (111) plane showed the strongest XRD peak. This plane shows the strongest XRD peak in Al alloys. However, with the effect of the coating, it was observed that the most intense XRD peak was in the (200) plane.  $\gamma\text{-Al}_2\text{O}_3$  on the coating surface intensely peaks at 39.4, 45.7, and 66.7 degrees. There is  $\gamma\text{-Al}_2\text{O}_3$  at 39.4° (222), 45.7° (400) and 66.7° (440) plane. The existence of  $\text{Al}_2\text{O}_3$  coating, which we observed with microstructures, was proved by XRD analysis.



**Figure 3.** a) Schematic view of the discharge channels from the cross-section  
b) EDS analysis of coating zone



**Figure 4.** X-ray diffraction patterns of SM and S sample

The hardness values of the starting material Al 7075-T6 (S) and MAO coated samples (SM) are shown in Figure 5. The hardness of the (S) sample was measured as 180 HV0.5. The hardness of the micro arc coated sample (SM) was measured as 272 HV0.5.

It is known from the literature that the hardness of the coating will increase. However, although the 2μm coating was thin, the hardness value increased by about 50%. In order to examine the relationship between hardness value and dislocation density, dislocation densities were calculated by XRD analysis. In Figure 2, the

dislocation density values are given together with the hardness value. At the same time, crystallite size value was calculated while dislocation density calculations were made. The Crystallite size and dislocation density of the samples with the Debye Scherrer formula was calculated.

Debye Scherrer's equation;

$$Dp = k * \lambda / \beta * \cos \theta \quad (1)$$

The dislocation density ( $\delta$ )

$$\delta = 1/Dp^2 \quad (2)$$

Crystallite sizes calculated with the FWHM value obtained by XRD analysis; It was found to be  $611.8 \cdot 10^{-10}$  m in the S sample and  $568.2 \cdot 10^{-10}$  m in the SM sample. The crystallite size of the coated sample decreased. It is thought that the grain form changes due to diffusion during coating. Therefore, Figure 2 shows that the dislocation density of the coated sample also increased. At the same time, while coating is being done, the atoms tend to move towards the surface during diffusion. Thus, crystal structure errors occur. It is thought that these faults lock the dislocations and increase the hardness.

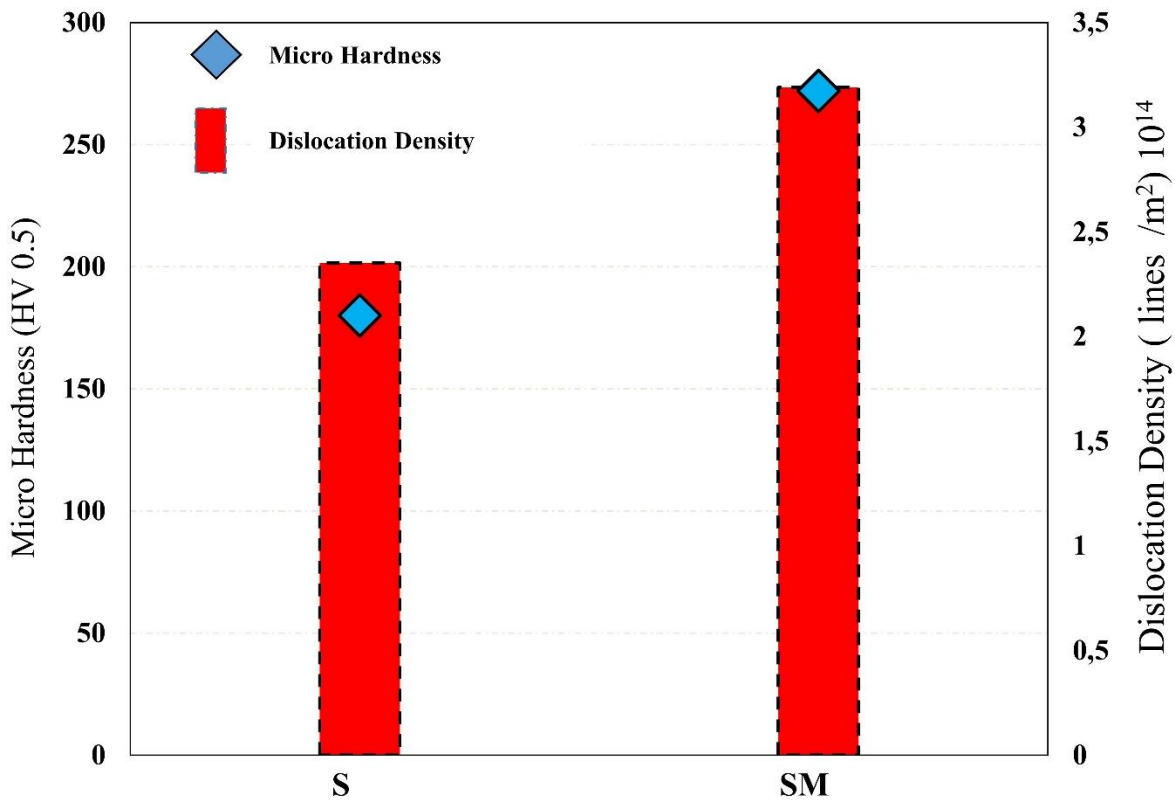


**Figure 5.** Microhardness results and dislocation densities of samples

Figure 6-7 and Table 2 show the wear test weight loss of the samples. In the experiments carried out to determine the wear performance, the test load and the total sliding distance were chosen as 5N, 10N, 15N and 500-1000-1500 m, respectively. When Table 2 is examined, it is possible to say that there is a relatively homogeneous weight loss depending on the unit distance. This homogeneity in weight losses is reflected as a linear increase in the slope of the graphs. We can say that the steepness of the slope is increased by the applied force. When the weight losses are examined, the fact that the weight loss of the sample with 2  $\mu$ m coating thickness applied 5N load is the least compared to the other coated samples can be attributed to the stronger interfacial bond strength. Based on this, other samples with micro arc coated 10N and 15N loads support this

result. The SEM image of the SM sample, as examined in Figure 6, supports the image of the weight loss caused by the applied 5N load. When the traces formed were examined, it was determined that the wear lines became more pronounced due to the increasing weight. In Figure 7, wear graphs of the S sample are shown. With the applied coating, the wear behavior of the material is directly affected by its mechanical and structural properties. The MAO coating showed significant wear resistance compared to its uncoated state. According to the wear test results, it was determined that the wear marks of the samples applied with 5N test load were less than the samples applied with 10N and 15N test loads. Based on this, according to the sample SEM results, the wear marks increased with the increase in the test load. The visible white coatings on the MAO 2 $\mu$ m 15N surface are thought to have been re-adhered to the surface of the broken pieces. It shows that the weight loss of the SM sample with increasing test loads is less compared to the S sample and thus its wear resistance is higher. Compared to the S sample, the abrasion resistance of the SM sample increased approximately 8 times at 5N load, 10 times at 10N and 7.5 times at 15N load.

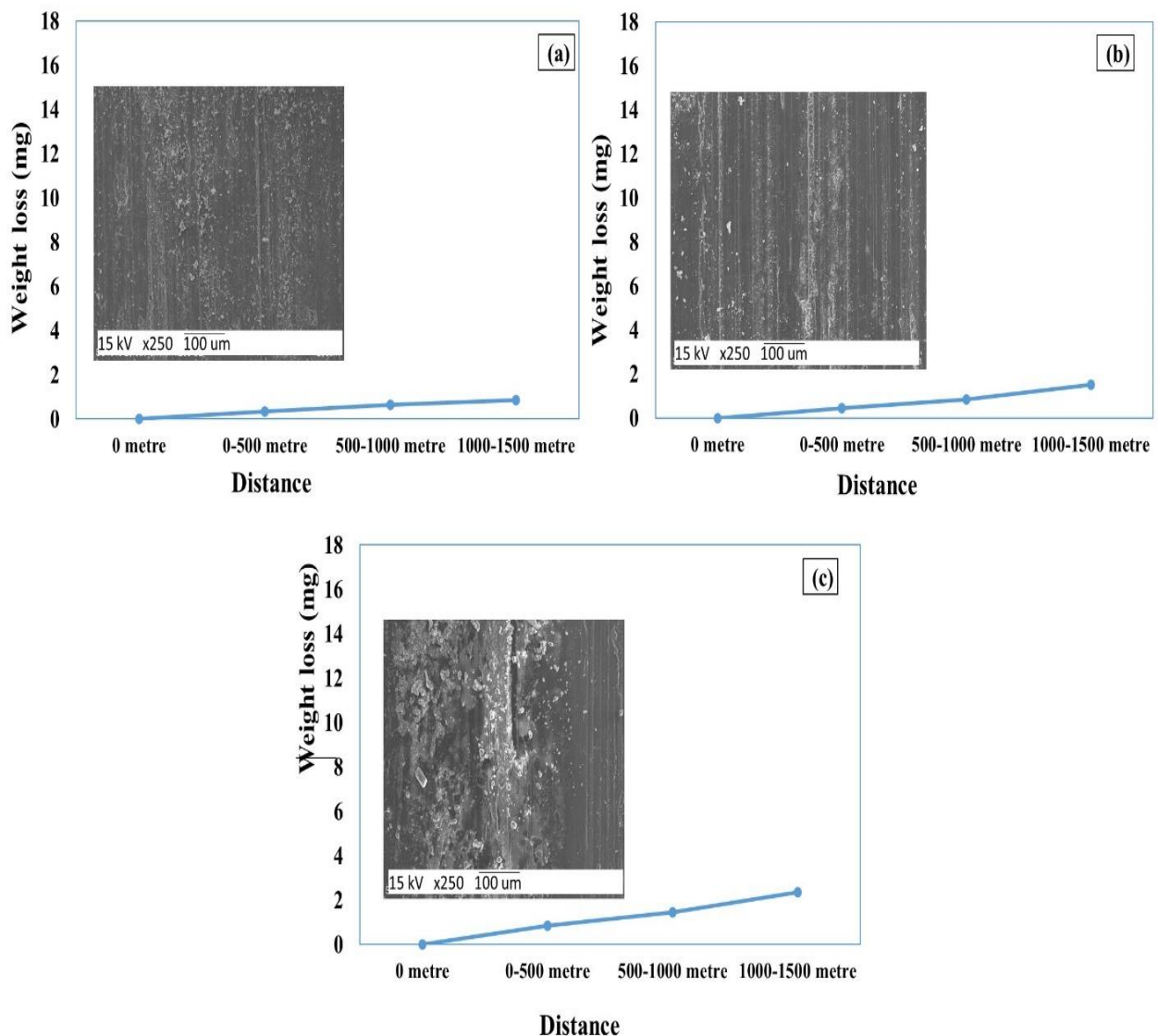


**Figure 6.** Abrasion test weight loss graphs of SM (7075-T6 Al+MAO) sample at a) 5N b) 10N c) 15N loads

Figure 8 shows the friction coefficient-distance graph of the samples. The friction coefficient of the SM sample was 0.2, and the friction coefficient of the S sample was 0.5. The fact that the SM sample has less friction coefficient indicates that the abrasion resistance is better.

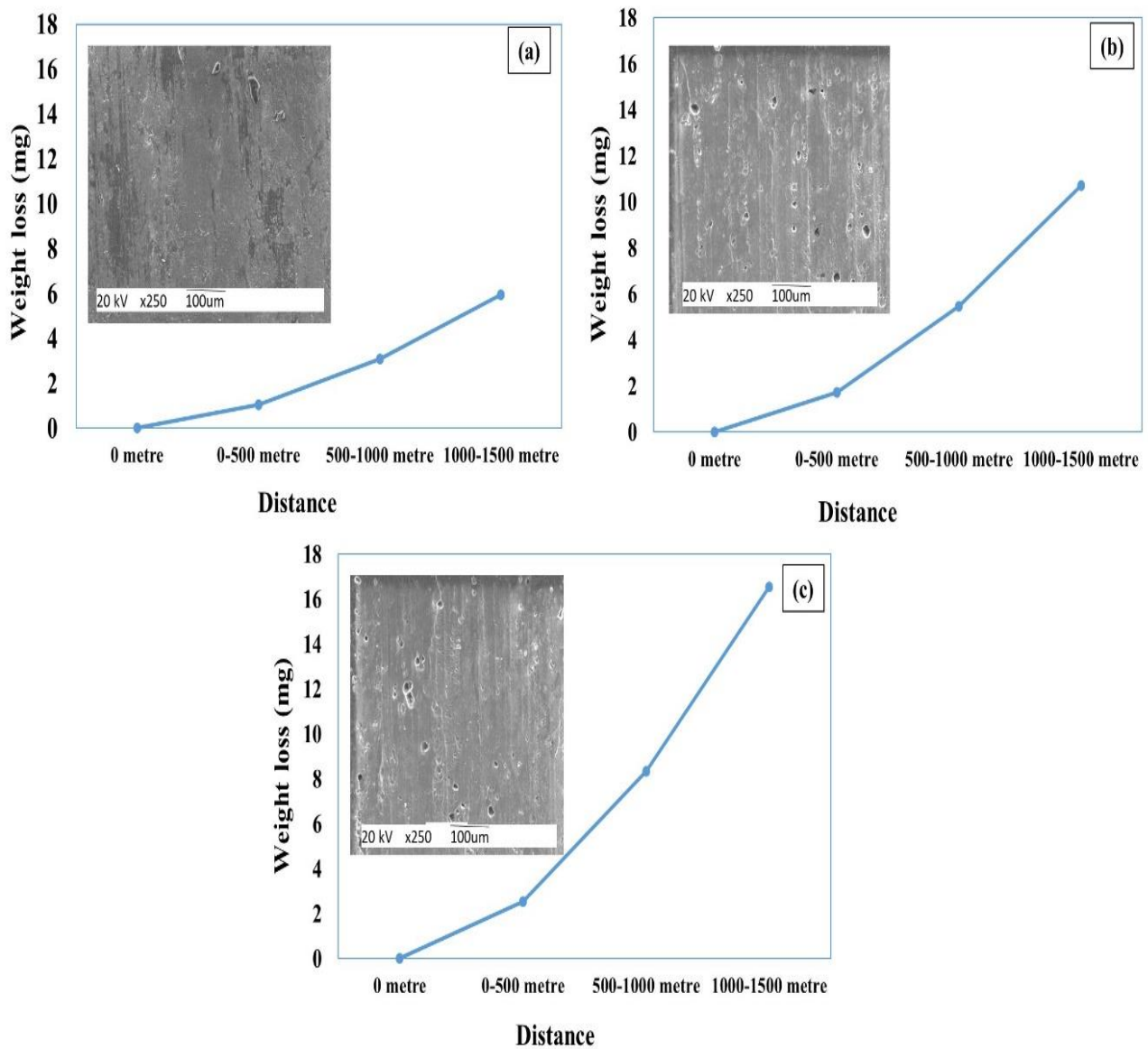
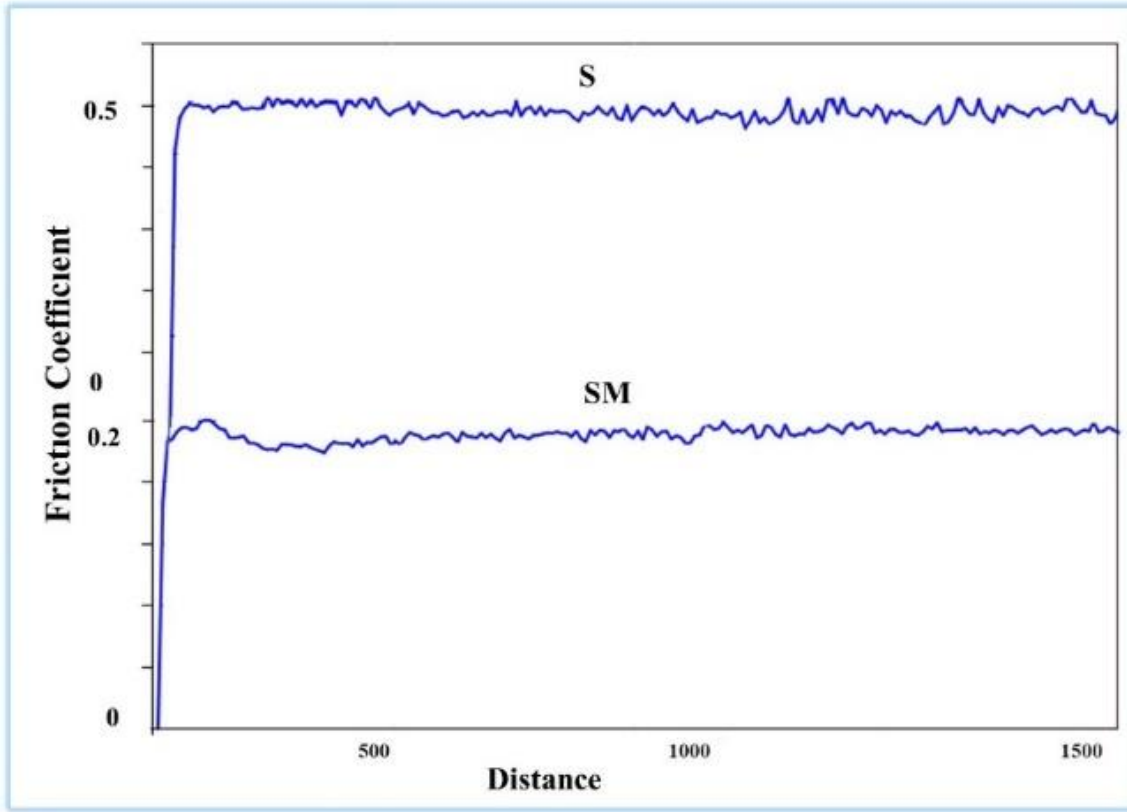


Figure 7. Abrasion test weight loss graphs of S (7075-T6 Al) sample a)5N b)10N c)15N loads

Table 2. Wear test weight loss results of SM and S samples

Material	Weight Loss			
	0-500 metre	500-1000 metre	1000-1500 metre	Total Weight
SM 2µm 5N	0,33 mg	0,31 mg	0,21 mg	0,85 mg
SM 2µm 10N	0,45 mg	0,38 mg	0,67 mg	1,50 mg
SM 2µm 15N	0,83 mg	0,61 mg	0,9 mg	2,34 mg
S 5N	1,04 mg	2,05 mg	2,85 mg	5,94 mg
S 10N	1,74 mg	3,71 mg	5,27 mg	10,72 mg
S 15N	2,52 mg	5,81 mg	8,22 mg	16,55 mg



**Figure 8.** Friction coefficient values of SM and S samples

#### 4. CONCLUSION

In this study, a very thin 2 micron MAO coating was applied to the Al 7075-T6 alloy to reduce the cost. The following results were obtained

- The hardness of the MAO-coated samples increased by 50% compared to the uncoated samples.
- Although the coating thickness of the sample that was coated on the aluminum 7075-T6 surface was so thin, the wear resistance increased 8 times compared to the uncoated sample.
- The friction coefficient of the sample coated with MAO is lower than the Al 7075-T6 sample.
- By coating the samples with MAO, the average pore diameters are 1.48  $\mu\text{m}$ .

#### ACKNOWLEDGMENT

This research was supported by the Gazi University BAP unit with the project number FDK-2023-7620.

#### CONFLICT OF INTEREST

The authors declare no conflict of interest.

#### REFERENCES

Altuntaş, O. (2022). Enhancement of impact toughness properties of Al 7075 alloy via double aging heat treatment. *Gazi University Journal of Science Part C: Design and Technology*, 10(2), 194-202. doi:[10.29109/gujsc.1108116](https://doi.org/10.29109/gujsc.1108116)

Altuntaş, O., & Güral, A. (2015). Yüksek Karbonlu Sinterlenmiş Çeliklerin Darbe Tokluklarına Küreselleştirme Isıl İşlemlerinin Etkisinin İncelenmesi [Examining Effect of Speheroidization Heat Treatments on Impact Toughness of High Carbon Sintered Steel]. *Politeknik Dergisi*, 18(3), 107-112.

- Altuntaş, G., Altuntaş, O., & Bostan, B. (2021). Characterization of Al-7075/T651 Alloy by RRA Heat Treatment and Different Pre-deformation Effects. *Transactions of the Indian Institute of Metals*, 74(12), 3025-3033. doi:[10.1007/s12666-021-02369-5](https://doi.org/10.1007/s12666-021-02369-5)
- Baxi, J., Kar, P., Liang, H., Polat, A., Usta, M., & Uçışık, A. H. (2008) Tribological characterization of microarc oxidized alumina coatings for biological applications. *Vacuum*, 83(1), 217-222. doi:[10.1016/j.vacuum.2008.03.085](https://doi.org/10.1016/j.vacuum.2008.03.085)
- Dean, J., Gu, T., & Clyne, T. W. (2015). Evaluation of residual stress levels in plasma electrolytic oxidation coatings using a curvature method. *Surface and Coatings Technology*, 269, 47-53. doi:[10.1016/j.surfcoat.2014.11.006](https://doi.org/10.1016/j.surfcoat.2014.11.006)
- Hussein, R. O., Nie, X., & Northwood, D. O. (2013). An investigation of ceramic coating growth mechanisms in plasma electrolytic oxidation (PEO) processing. *Electrochimica Acta*, 112, 111-119. doi:[10.1016/j.electacta.2013.08.137](https://doi.org/10.1016/j.electacta.2013.08.137)
- Li, Z.-y., Cai, Z.-b., Cui, Y., Liu, J.-h., & Zhu, M.-h. (2019). Effect of oxidation time on the impact wear of micro-arc oxidation coating on aluminum alloy. *Wear*, 426-427(A) 285-295. doi:[10.1016/j.wear.2019.01.084](https://doi.org/10.1016/j.wear.2019.01.084)
- Qi, X., Song, R., Wang, C., & Jiang, B. (2022). Influence of Interfacial Stress Produced by MAO on Electrochemical Corrosion and Stress Corrosion Cracking Behavior in 7075 Aluminum Alloy, *Journal of The Electrochemical Society*, 169(2), 020559. doi:[10.1149/1945-7111/ac534b](https://doi.org/10.1149/1945-7111/ac534b)
- Schneider, C. A., Rasband, W. S., & Eliceiri, K. W. (2012). NIH Image to ImageJ: 25 years of image analysis. *Nature Methods*, 9(7) 671-675. doi:[10.1038/nmeth.2089](https://doi.org/10.1038/nmeth.2089)
- Shen, Z., Wu, Z., Wang, T., Jia, T., & Liu, C. (2023). Research on Technology of 7075 Aluminum Alloy Processed by Variable Polarity TIG Additive Manufacturing Utilizing Nanoparticle-Reinforced Welding Wire with TiB<sub>2</sub>. *Crystals*, 13(3), 399. doi:[10.3390/cryst13030399](https://doi.org/10.3390/cryst13030399)
- Sobolev, A., Peretz, T., & Borodianskiy, K. (2020). Fabrication and characterization of ceramic coating on Al7075 Alloy by plasma electrolytic oxidation in molten salt. *Coatings*, 10(10), 993. doi:[10.3390/coatings10100993](https://doi.org/10.3390/coatings10100993)
- Song, G.-L., & Shi, Z. (2014). Corrosion mechanism and evaluation of anodized magnesium alloys. *Corrosion Science*, 85, 126-140. doi:[10.1016/j.corsci.2014.04.008](https://doi.org/10.1016/j.corsci.2014.04.008)
- Sundararajan, G., & Krishna, L. R. (2003). Mechanisms underlying the formation of thick alumina coatings through the MAO coating technology. *Surface and Coatings Technology*, 167(2-3), 269-277. doi:[10.1016/S0257-8972\(02\)00918-0](https://doi.org/10.1016/S0257-8972(02)00918-0)
- Xin, S.-G., Song, L.-X., Zhao, R.-G., & Hu, X.-F. (2006). Composition and thermal properties of the coating containing mullite and alumina. *Materials Chemistry and Physics*, 97(1), 132-136. doi:[10.1016/j.matchemphys.2005.07.073](https://doi.org/10.1016/j.matchemphys.2005.07.073)
- Yılmaz, M. S., Özer, G., Şahin, O., & Karaaslan, A. (2021). Investigation of the Effects of Different Retrogression and Re-Aging Parameters Applied to the 7075 Alloy on the Micro-Arc Oxidation Process. *Surface Review and Letters*, 28(09), 2150078. doi:[10.1142/S0218625X21500785](https://doi.org/10.1142/S0218625X21500785)
- Zhang, J., Dai, W., Wang, X., Wang, Y., Yue, H., Li, Q., Yang, X., Guo, C., & Li, C. (2023). Micro-arc oxidation of Al alloys: Mechanism, microstructure, surface properties, and fatigue damage behavior. *Journal of Materials Research and Technology*, 23, 4307-4333. doi:[10.1016/j.jmrt.2023.02.028](https://doi.org/10.1016/j.jmrt.2023.02.028)